Available online at www.sciencedirect.com
ScienceDirect
Journal of Sound and Vibration 324 (2009) 903–915
JOURNAL OF SOUND AND VIBRATION
www.elsevier.com/locate/jsvi

A numerical study of the nonlinear dynamics of a light, axially moving band in surrounding fluid

H. Koivurova*, J. Laukkanen

Department of Mechanical Engineering, University of Oulu, Box 4200, FIN-90014 University of Oulu, Finland

Received 4 August 2008; received in revised form 9 February 2009; accepted 10 February 2009
Handing Editor: A.V. Metrikine
Available online 10 March 2009

Abstract

The vibration characteristics of a submerged axially moving band are investigated by a numerical study. A geometrically nonlinear axially moving band model is coupled to the acoustic fluid model and the periodic nonlinear problem is solved by the Fourier–Galerkin–Newton (FGN) method. The nonlinear dynamic behaviour is examined through the dependences between fundamental frequency, axial velocity and the amplitude of nonlinear free vibration. The results are compared with the behaviour of an axially moving band in a vacuum as considered in the companion paper [H. Koivurova, *Journal of Sound and Vibration* 320 (2009) 373–385]. In the subcritical speed range the system behaved as expected, in that the effect of the surrounding air field reduced the fundamental frequency to about one fifth of the vibration observed in a vacuum. In the supercritical speed range the effects of the surrounding air depended on the amplitude of vibration and its change with increasing geometrical nonlinearity. With linear vibrations the fundamental frequency grows faster as a function of axial velocity than in vacuum, but with nonlinear vibrations the increase in frequency is slower than in a vacuum at near-critical velocities, but with a tendency to increase faster at higher velocities.

1. Introduction

There is a large class of industrial processes which involve the transport of bands and webs across spans. From the point of view of mechanics, the translating structural members must have special characteristics with regard to vibration and dynamic stability. The topic of axially moving material has been studied widely, and recent research developments have been reviewed by Chen [1] and Païdoussis [2]. Our interest is in the topic of nonlinear vibrations in an axially moving string, which has also received much attention. An extensive literature overview can be found in companion paper [3].

The paper making process, for instance, often includes high-speed operations in which a thin, light web interacts closely with the surrounding air flow, causing out-of-plane vibrations, or flutter. Theoretical and experimental results show that the effects of the surrounding air on the dynamic behaviour of a paper web are significant. According to the experimental results of Pramila [4], the critical velocities and natural frequencies

*Corresponding author. Tel.: +358 8 553 2172; fax: +358 8 553 2026.
E-mail addresses: Hannu.Koivurova@oulu.fi (H. Koivurova), Jari.Laukkanen@oulu.fi (J. Laukkanen).

0022-460X/$ - see front matter © 2009 Elsevier Ltd. All rights reserved.
doi:10.1016/j.jsv.2009.02.011

are only 15–30% of the values given by predictions that neglect the interaction between the paper sheet and the surrounding air.

The first analyses of flutter in a moving web were performed by Pramila [5] and Chang et al. [6] using analytical "travelling thread line" models but neglecting the cross-direction variation in web motion by assuming that the entire web width deflects uniformly. The motion of the surrounding air was taken into account as an ideal fluid in various added mass models. These analytical studies confirmed the importance of the surrounding air for light webs and showed that it affects the eigenfrequencies and critical speed of the web. The viscous flow of the air particles was included in the above model by Frondelius et al. [7], who used an analytical model of a boundary layer on moving continuous flat surfaces to demonstrate that the viscous boundary layer flow has a clear influence and that it grows with increasing axial velocity. The drop in the critical speed of the system can be significant due to turbulent flow if the span length of the system is high.

The dynamic behaviour of the interaction of a light structure with a surrounding air has been studied widely, e.g. in Refs. [8–10], but systems which also include axial motion of the structure have rarely been considered. In the first three dimensional studies the web was modelled as a linear membrane and the surrounding air treated as an incompressible ideal fluid by Niemi and Pramila [11] and as a compressible ideal fluid by Laukkanen and Pramila [12]. The geometrically nonlinear effect was included by Koivurova and Pramila [13] when they used a nonlinear membrane element to model a narrow axially moving band surrounded by air. The influence of air was accounted for with acoustic elements. Recently Kulachenko et al. [14] used geometrically nonlinear Mindlin shell elements and an orthotropic material model for the paper web and acoustic finite elements for modelling the surrounding air and showed that besides reducing the eigenfrequencies of the web, the surrounding air suppresses wrinkled modes with a low modal effective mass.

The aim of this work is to examine the subcritical and supercritical speed dynamics of an axially moving narrow band by considering the interaction between the moving band and the surrounding air in terms of a geometrically nonlinear structural model and a surrounding acoustic fluid. The equations of motion are formulated using the structural model of axially moving string developed in Ref. [3] and an acoustic fluid model for the surrounding air. The formulation of the problem leads to coupled equations of motion, but because of the large fluid domain and its many degrees of freedom, the size of the nonlinear problem is minimized by decomposition. The effect of the linear fluid domain is taken into account by means of the structure motion-dependent fluid pressure at the fluid-structure interface of the band. Moreover, the system matrices of the fluid domain are diagonalized by expressing them in terms of the modal coordinates. The nonlinear dynamic behaviour of the structure is investigated by analysing the free and steady-state periodic vibration of the geometrically nonlinear axially moving band. The periodic nonlinear problem is solved by the Fourier–Galerkin–Newton (FGN) method according to Narayanan and Sekar [15]. The structural response to harmonic excitations and the backbone curves of free vibration show that the nonlinearities and coupling phenomena have a considerable effect on the dynamic behaviour of the system and can be seen clearly if we compare the results with those applying to the system described in Ref. [3].

2. Theoretical formulation

The model of the system to be considered is shown in Fig. 1. The structural part, a light axially moving band, is modelled with a geometrically nonlinear string element that neglects the cross-direction variation in web motion by assuming that the entire web width deflects uniformly. The formulation of the structural model is presented in the first part of this work [3]. The surrounding fluid is modelled as an acoustic fluid using pressure formulation.

2.1. *Acoustic fluid*

The fluid is treated as a linear acoustic approximation, i.e. as a compressible, non-viscid, non-flowing medium. These assumptions lead to the well-known Helmholtz equation as shown in Ref. [16], for instance. Using a standard finite element procedure, the acoustic wave equations result in a set of discretized governing

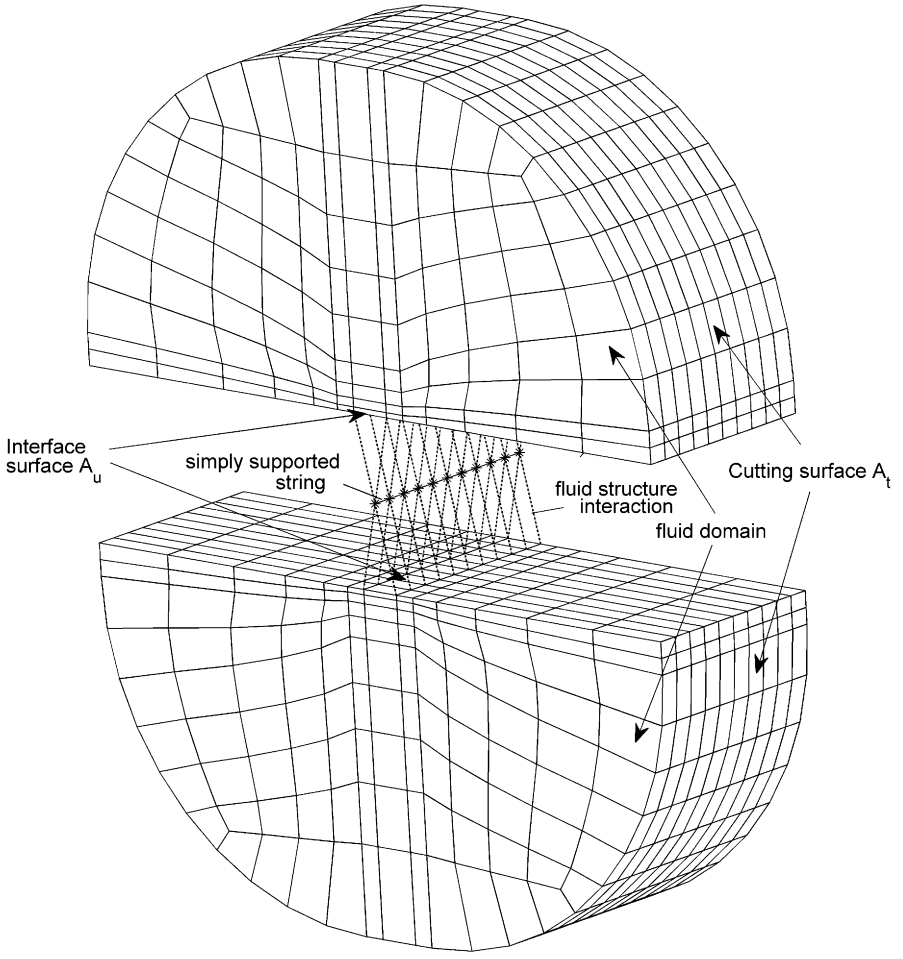

Fig. 1. Model of an axially moving narrow band in surrounding air.

equations [16,17]. The pressure distribution in the fluid domain V is approximated by

$$p(x,y,z) = \mathbf{N}^P \mathbf{p}, \tag{1}$$

where $\mathbf{N}^P$ is the shape function vector of a linear three-dimensional isoparametric 8 node element, and $\mathbf{p}$ is the nodal pressure vector. The discretized equation for the fluid domain V is then [16]

$$\mathbf{L}\ddot{\mathbf{p}} + \mathbf{D}\dot{\mathbf{p}} + \mathbf{H}\mathbf{p} = \mathbf{F}_p, \tag{2}$$

where the points denote derivates with respect to the time t and $\mathbf{L}$ is the fluid mass matrix

$$\mathbf{L} = \frac{1}{c^2}\int_V (\mathbf{N}^P)^{\mathrm{T}} \mathbf{N}^P \,\mathrm{d}V, \tag{3}$$

where c is the wave speed in fluid, $\mathbf{D}$ is the "damping" matrix arising from the radiation boundary condition at the cutting boundary A_t of the fluid

$$\mathbf{D} = \frac{1}{c}\int_{A_t} (\mathbf{N}^P)^{\mathrm{T}} \mathbf{N}^P \,\mathrm{d}A, \tag{4}$$

$\mathbf{H}$ is the fluid stiffness matrix

$$\mathbf{H} = \int_V (\nabla \mathbf{N}^P)^{\mathrm{T}} \nabla \mathbf{N}^P \,\mathrm{d}V, \tag{5}$$

and $\mathbf{F}_p$ is the external force vector of the fluid domain at the interface surface A_u

$$\mathbf{F}_p = \int_{A_u} (\mathbf{N}^P)^{\mathrm{T}} \frac{\partial p}{\partial n} \, \mathrm{d}A. \tag{6}$$

The fluid domain V, the cutting boundary surface A_t and the interface surface A_u are shown in Fig. 1.

2.2. Coupled equations of motion

The structural and fluid equations are coupled through their respective external force vectors [16]. The fluid pressure $\mathbf{p}$ at the fluid–structure interface translates to an external traction on the structure in the direction of the fluid normal $\mathbf{n}$, and the force vector is

$$\mathbf{F}_s = \mathbf{S}^{\mathrm{T}}\mathbf{p}. \tag{7}$$

where $\mathbf{S}$ is the interaction matrix at the interface surface A_u

$$\mathbf{S} = \int_{A_u} (\mathbf{N}^P)^{\mathrm{T}} \mathrm{n} \mathbf{N} \, \mathrm{d}A \tag{8}$$

and $\mathbf{N}$ is shape function matrix of the structural part, the geometrically nonlinear string element defined in Ref. [3]. The structural acceleration at the interface nodes $\ddot{\mathbf{q}}$ translates to the normal derivative of pressure on the fluid, and the force vector at the interface with the fluid is

$$\mathbf{F}_p = -\rho_f \mathbf{S}\ddot{\mathbf{q}}, \tag{9}$$

where ρ_f is fluid density. The coupling between the 3D fluid and string entails the assumption that the entire band width deflects uniformly, and therefore two nodes of the fluid in the width of the band are coupled to a spring node, as shown in Fig. 1. By defining A_u as the structural and fluid surface at the interface, the finite element equations for the coupled system can be expressed with the help of Ref. [3] as

$$\begin{bmatrix} \mathbf{M} & 0 \\ \rho_f \mathbf{S} & \mathbf{L} \end{bmatrix} \begin{Bmatrix} \ddot{\mathbf{q}} \\ \ddot{\mathbf{p}} \end{Bmatrix} + \begin{bmatrix} \mathbf{C} & 0 \\ 0 & \mathbf{D} \end{bmatrix} \begin{Bmatrix} \dot{\mathbf{q}} \\ \dot{\mathbf{p}} \end{Bmatrix} + \begin{bmatrix} \mathbf{K}(\mathbf{q}) & -\mathbf{S}^{\mathrm{T}} \\ 0 & \mathbf{H} \end{bmatrix} \begin{Bmatrix} \mathbf{q} \\ \mathbf{p} \end{Bmatrix} = \begin{Bmatrix} \mathbf{F}(t) \\ 0 \end{Bmatrix}, \tag{10}$$

where $\mathbf{q}$ is the vector with the nodal structural displacements of the axially moving string, $\mathbf{M}$ is the mass matrix, $\mathbf{C}$ is the damping matrix, $\mathbf{K}(\mathbf{q})$ is the nonlinear stiffness matrix of the axially moving string and $\mathbf{F}$ is the force vector of the axially moving string.

3. Periodic solution for the coupled system

The dynamic response of the system is assumed to be periodic with a frequency of ω. Using non-dimensional time $\tau = \omega t$, the equation of the motion, Eq. (10) becomes

$$\omega^2 \mathbf{M}_c \mathbf{x}'' + \omega \mathbf{C}_c \mathbf{x}' + \mathbf{K}_c(\mathbf{q})\mathbf{x} = \mathbf{F}_c(\tau), \tag{11}$$

where the primes denotes derivates with respect to the non-dimensional time τ and subscript c denotes that the terms are matrices and vectors of the coupled fluid–structure interaction system shown in Eq. (10) and $\mathbf{x}$ contain the displacement of the string and the pressure of the fluid field. Following the FGN procedure described in Ref. [3], the equation of motion is obtained as

$$\overline{\mathbf{K}}\Delta\mathbf{X} = \overline{\mathbf{R}} - \overline{\mathbf{R}}_{\omega}\Delta\omega, \tag{12}$$

where

$$\overline{\mathbf{K}} = \omega_0^2 \overline{\mathbf{M}}_c + \omega_0 \overline{\mathbf{C}}_c + \overline{\mathbf{K}}_{cT}(\mathbf{q}_0),$$

$$\overline{\mathbf{R}} = \overline{\mathbf{F}}_c - [\omega_0^2 \overline{\mathbf{M}}_c + \omega_0 \overline{\mathbf{C}}_c + \overline{\mathbf{K}}_c(\mathbf{q}_0)]\mathbf{X},$$

$$\overline{\mathbf{R}}_{\omega} = (2\omega_0\overline{\mathbf{M}}_c + \overline{\mathbf{C}}_c)\mathbf{X}, \tag{13}$$

$\overline{\mathbf{M}}_c, \overline{\mathbf{C}}_c$, $\overline{\mathbf{K}}_{cT}$ and $\overline{\mathbf{F}}_c$ are obtained either through FFT or DFT, as shown in Ref. [3].

3.1. Modelling the fluid as a pressure loading

The above formulation of the problem leads to the coupled equations of motions Eq. (12), but because of the large fluid domain and its many degrees of freedom, the size of the problem is minimized by decomposing it into a nonlinear structural part and a linear fluid part, and the equation of motion Eq. (11) becomes

$$\omega^2\mathbf{M}\mathbf{q}'' + \omega\mathbf{C}\mathbf{q}' + \mathbf{K}(\mathbf{q})\mathbf{q} = \mathbf{S}^{\mathrm{T}}\mathbf{p} + \mathbf{F}(\tau),$$

$$\omega^2\mathbf{L}\mathbf{p}'' + \omega\mathbf{D}\mathbf{p}' + \mathbf{H}\mathbf{p} = -\omega^2\rho_f\mathbf{S}\mathbf{q}''. \tag{14}$$

Since a periodic solution is sought, the solution $\mathbf{p}$ is represented as Fourier series, i.e.

$$\mathbf{p} = \mathbf{P}_0 + \sum_{j=1}^{M}[\mathbf{P}_{2j-1}\cos(\mathrm{j}\tau) + \mathbf{P}_{2j}\sin(\mathrm{j}\tau)], \tag{15}$$

where $\mathbf{P}_0$ and $\mathbf{P}_j$'s are Fourier coefficients and M represents the number of harmonics.

Following the Galerkin procedure described in Ref. [3] for the fluid part of the governing equation in Eq. (14), the following expression is obtained in the frequency domain:

$$\mathbf{K}_p(\omega)\mathbf{P} = \mathbf{F}_p(\omega, \mathbf{q}''), \tag{16}$$

where

$$\mathbf{K}_p(\omega) = \omega^2\mathbf{L} + \omega\mathbf{D} + \mathbf{H}, \tag{17}$$

$\mathbf{F}_p$ is the external force vector due to structural acceleration at the same interface as in Eq. (9), i.e.

$$\mathbf{F}_p = -\omega\rho_f\mathbf{S}\mathbf{q}'', \tag{18}$$

and $\mathbf{P} = \{\mathbf{P}_0, \mathbf{P}_1, \ldots, \mathbf{P}_{2M}\}^{\mathrm{T}}$. The force vector of the structural part at the fluid–structure interface attributable to the fluid pressure can be obtained by substituting Eqs. (16) and (18) into Eq. (7), and is

$$\mathbf{F}_s = -\omega^2\rho_f\mathbf{S}^{\mathrm{T}}\mathbf{K}_p^{-1}\mathbf{S}\mathbf{q}''. \tag{19}$$

By substituting Eq. (19) into the structural part of Eq. (14) the governing equation of the system becomes

$$\omega^2\mathbf{M}\mathbf{q}'' + \omega\mathbf{C}\mathbf{q}' + \mathbf{K}(\mathbf{q})\mathbf{q} + \omega^2\rho_f\mathbf{S}^{\mathrm{T}}\mathbf{K}_p^{-1}\mathbf{S}\mathbf{q}'' = \mathbf{F}(\tau). \tag{20}$$

Using the Newton–Raphson procedure with Taylor series expansion and the incrementation $\mathbf{q} = \mathbf{q}_0 + \Delta\mathbf{q}$ and $\omega = \omega_0 + \Delta\omega$, we obtain the linearized incremental equation

$$\begin{aligned}\omega^2\mathbf{M}\Delta\mathbf{q}'' + \omega\mathbf{C}\Delta\mathbf{q}' + \mathbf{K}_T(\mathbf{q})\Delta\mathbf{q} + \omega^2\rho_f\mathbf{S}^{\mathrm{T}}\mathbf{K}_P^{-1}\mathbf{S}\Delta\mathbf{q}''\\ = \mathbf{R} - (2\omega_0\mathbf{M}\mathbf{q}_0'' + \mathbf{C}_c\mathbf{q}_0' + 2\omega\rho_f\mathbf{S}^{\mathrm{T}}\mathbf{K}_P^{-1}\mathbf{S}\mathbf{q}_0'')\Delta\omega,\end{aligned} \tag{21}$$

where the residual is

$$\mathbf{R} = \mathbf{F}(\tau) - [\omega_0^2\mathbf{M}\mathbf{q}_0'' + \omega_0\mathbf{C}\mathbf{q}_0' + \mathbf{K}(\mathbf{q}_0)\mathbf{q}_0 + \omega^2\rho_f\mathbf{S}^{\mathrm{T}}\mathbf{K}_p^{-1}\mathbf{S}\mathbf{q}_0'']. \tag{22}$$

Following the FGN procedure described in Ref. [3] for the Eq. (21), the equation of motion is obtained in which the effect of the surrounding air is taken into account by means of the structure motion-dependent fluid pressure at the fluid-structure interface of the band.

From Eq. (17) it can be seen that the matrix $\mathbf{K}_p$ is dependent on the frequency ω, and therefore the inverse of $\mathbf{K}_p$ should calculate every iteration of a Newton–Raphson procedure in terms of changes in the frequency ω. In order to reduce the computation, the equations for the fluid domain are transformed to modal coordinates, i.e.

$$\mathbf{\Phi}^{\mathrm{T}}\mathbf{L}\mathbf{\Phi} = \mathbf{\Lambda},$$

$$\mathbf{\Phi}^{\mathrm{T}}\mathbf{D}\mathbf{\Phi} = \mathbf{\Lambda},$$

$$\mathbf{\Phi}^{\mathrm{T}}\mathbf{H}\mathbf{\Phi} = \mathbf{\Theta},$$

$$\mathbf{\Phi}^{\mathrm{T}}\mathbf{S} = \mathbf{\Sigma}, \tag{23}$$

where $\mathbf{\Phi}$ is the matrix of the L-orthogonal eigenvectors of the fluid domain, $\mathbf{\Lambda}$ is the diagonal matrix of the modal masses, $\mathbf{\Delta}$ is the diagonal matrix of the modal damping due to the radiation boundary condition at the cutting boundary A_t, $\mathbf{\Theta}$ is the diagonal matrix of the modal stiffnesses and $\mathbf{\Sigma}$ is the transformed interaction matrix. The transformation will reduce $\mathbf{K}_p$ of Eq. (21),

$$\mathbf{\Phi}^{\mathrm{T}}\mathbf{K}_p\mathbf{\Phi} = \omega^2\mathbf{\Lambda} + \omega\mathbf{\Delta} + \mathbf{\Theta}, \tag{24}$$

to the diagonal form and calculation of the inverse of the matrix is replaced by divisions of the diagonal terms.

4. Results

4.1. Verification

It is quite difficult to verify the overall accuracy of the model because there are only a few experimental results which consider axially moving bands and these are limited to a linear range of displacement. Pramila [4] measured the fundamental frequencies of a narrow paper web using a pilot coater with a web length of $L = 2.4$ m, width of $b = 0.47$ m and weight per unit length of $m = 17$ g/m. These values are used in the current model for an axially moving narrow band with the simple fixed supports and the dimensions and boundary conditions of the air domain given in Niemi and Pramila [11] and Laukkanen and Pramila [12]. The following additional parameters are used: thickness of the band $h = 0.49$ mm, initial tension $T_0 = 170$ N and Young's modulus $E = 1 \times 10^9$ N/m^2.

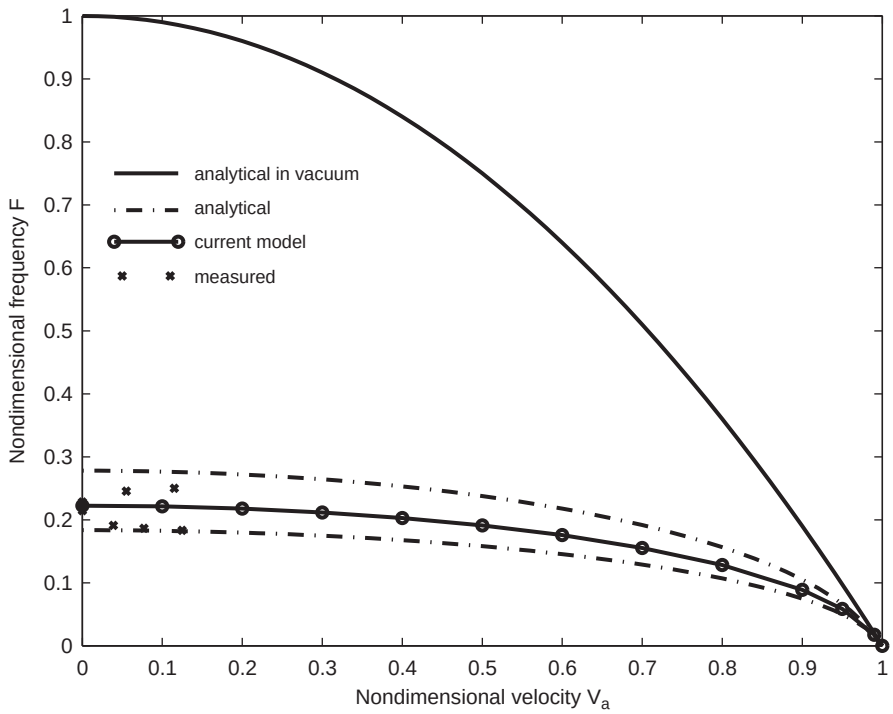

Fig. 2. Non-dimensional fundamental frequency F as a function of non-dimensional axial velocity V_a.

The results of the analysis of free vibration in the case of the numerical model and the experiments performed by Pramila [4] are shown in Fig. 2. The two dashed lines represent analytical results of Pramila [5], in which the surrounding air is described using two different added mass models. For the sake of clarity the results are shown in non-dimensional form, where the frequency is presented relative to the fundamental analytical frequency f_{l0} and the axial velocity relative to the critical velocity $v_{a(cr)}$. These are defined as follows:

$$F = f2L\sqrt{\frac{m}{T_0}} = f/f_{l0}, \tag{25}$$

$$V_a = v_a\sqrt{\frac{m}{T_0}} = v_a/v_{a(cr)}. \tag{26}$$

The same non-dimensional presentation is used for all the following analyses. The current results shown in Fig. 2 are in good agreement with the analytical results of when interaction with the air is taken into account. Also the few measured points confirm the current results.

4.2. Effects of decomposition and modal superposition of the model

Solution of the nonlinear problem in the coupled fluid–structure interaction model is labourious, because the fluid model is large. The response of a harmonic force situated in the middle of the simply supported axially moving band is solved with the coupled fluid–structure interaction model in Fig. 1 by using the same parameters as for the linear verification application above when the non-dimensional velocity is $V_a = 0.5$. The response curves are shown in Fig. 3. The curve AB is used as a basis for comparing the decomposition and modal superposition models explained in Section 3.1. At the same time we have considered the effect of boundary damping on the air domain. The percentual difference in frequency between the base curve of the fully coupled model and the other models with and without boundary damping is presented as a function of non-dimensional amplitude in Fig. 4. If we examine the full model we can see that the boundary damping

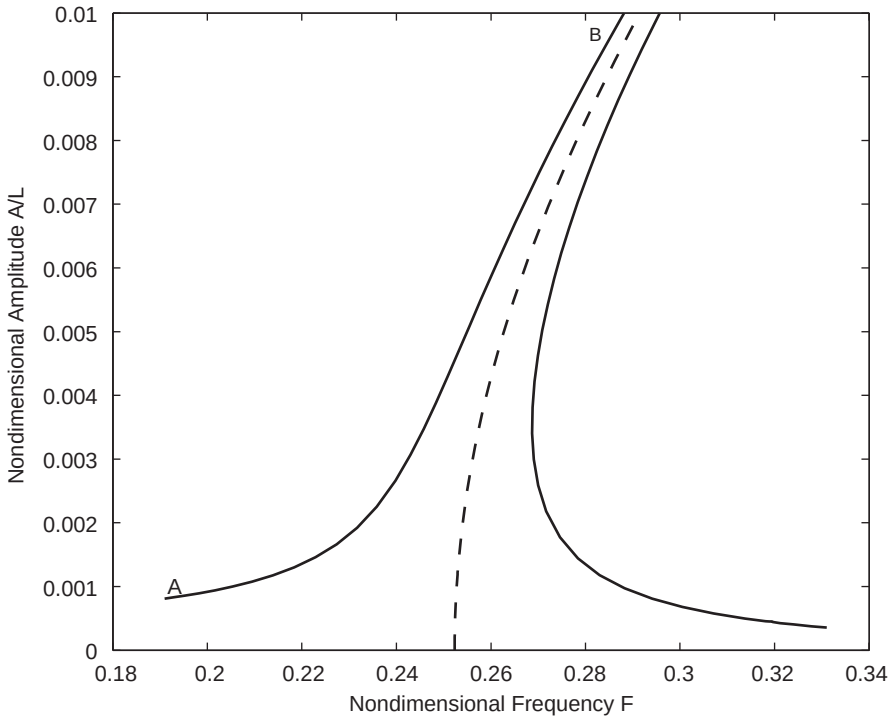

Fig. 3. Non-dimensional mid-span response amplitude for non-dimensional velocity of 0.5 travelling band excited with harmonic force near fundamental natural frequency. Results are calculated with full coupled fluid–structure interaction model.

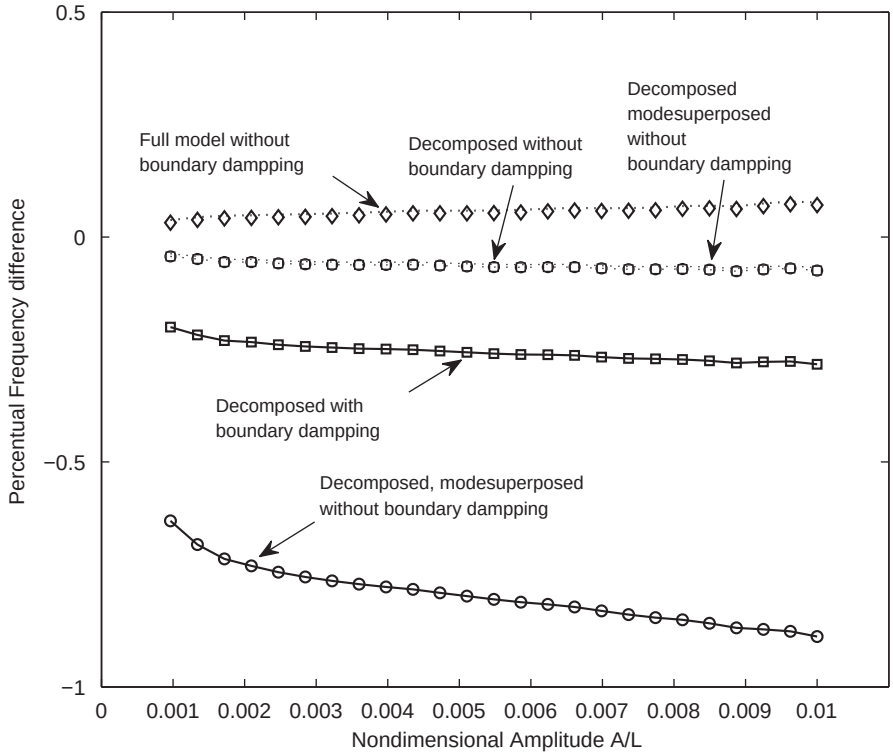

Fig. 4. Percentual difference in frequency between response of the full coupled model (curve *AB* of Fig. 3) and the other models with and without boundary damping as a function of non-dimensional amplitude.

increases the frequencies. This is an abnormal influence of damping on the normal structure, but for the coupled system the fluid–structure coupling operates through mass and stiffness, as shown in Eq. (10), and the cause and effect relation is not so simple. By comparing the full model with the decomposition and modal superposition models we see that without boundary damping they give accurate results with almost no difference between them. The use of the boundary damping clearly produces errors both in decomposition and in modal superposition, but these still remain less than one percent. The results of the modal superposed model are calculated in Fig. 4 by taking into account all the modes of eigenvalue analysis of the fluid domain, while the effect of the number of modes on the results is presented in Fig. 5. It is evident that accuracy demands the use of all the fluid domain eigenmodes.

The cpu times required for the different models are shown in Table 1. The fluid model includes 2860 degrees of freedom, the structure model 22 and the number of harmonic terms in the Fourier series is chosen to be 8. This means that the nonlinear equations have 48 994 degrees of freedom. Decomposition of the model into a linear fluid model and a nonlinear structure as explained in Section 3.1 will reduce the cpu time to one hundredth and modal superposition including all the modes will reduce it to one thousandth. It was found here that modal analysis needs to be done only once for the fluid model, so that it is not taken into account in the comparison.

4.3. *Fundamental frequency of free vibration*

The nonlinear dynamic behaviour of an axially moving band with surrounding air is examined through the dependences between fundamental frequency, axial velocity and the amplitude of nonlinear free vibration. The results are also compared with the behaviour of the same system in a vacuum as studied in the first part of this paper [3]. The parameters used are the same as in previous applications. The number of harmonics in the Fourier series is chosen on the basis of the value of the error estimate ε_2 as presented by Narayanan and Sekar

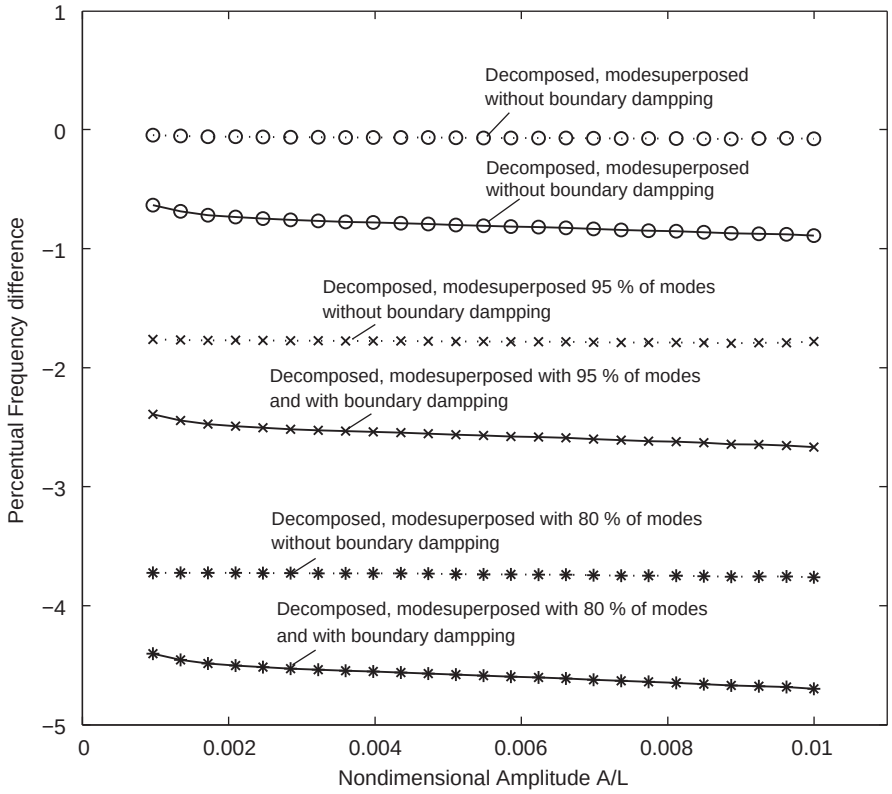

Fig. 5. Percentual difference in frequency between response of the full coupled model (curve AB of Fig. 3) and the decomposed and mode superposed models with different number of fluid eigenmodes included as a function of non-dimensional amplitude.

Table 1
The cpu-times of the different model solutions.

Model	cpu-time (s)[a]
Full coupled	86 873
Decomposed	862
Decomposed and mode superposed	(378)
Modal analysis	(294)
Periodic solution	84

[a]Matlab R2007b, Dell PowerEdge R900 with four 2.4 GHz quad core Xeon (E7330) and red Hat 4 AS.

[15] to indicate the magnitude of higher harmonic coefficients beyond the harmonic number. The criteria used for increasing the harmonic terms was $\varepsilon_2 = 0.1$, which led to numbers of harmonics between 4 and 32.

The backbone curves describing the relation between the non-dimensional amplitude ($= A/L$) of vibration and the non-dimensional fundamental frequency at different non-dimensional axial velocities are shown in Fig. 6. The curves for the system with air included do not differ much in shape at subcritical velocities ($V_a < 1$) from those of the system in a vacuum as shown in Fig. 5 of Ref. [3], as both systems behave in the manner of a nonlinear hard spring, but the magnitude of the frequencies was reduced to about one fifth, as observed in earlier linear studies (see Refs. [5,11]). In the supercritical velocity range ($V_a > 1$), however, the surrounding air has a much stronger influence on both the shapes and the magnitudes of the backbone curves. The system is still softening, but the effect of the surrounding air is the inverse of that observed at subcritical velocities as far as low amplitude values are concerned. The frequency of free vibration at the linear limit ($A/L = 0$) is $F = 0.17$ at an axial velocity $V_a = 1.03$ in air, while it is $F = 0.1$ for $V_a = 1.05$ in a vacuum [3]. Thus the

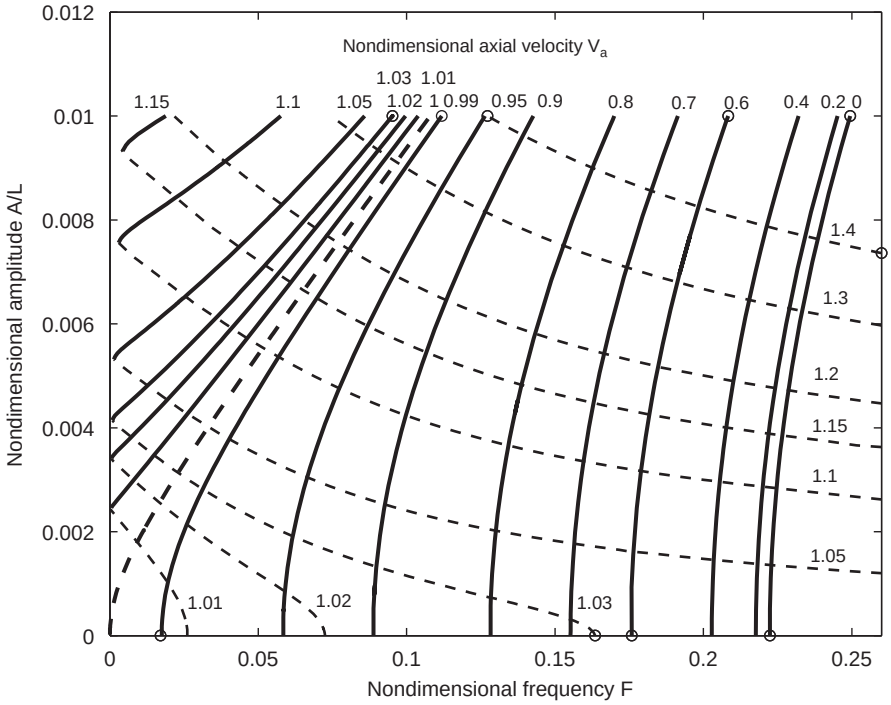

Fig. 6. Non-dimensional amplitude A/L as a function of non-dimensional fundamental frequency F with different non-dimensional axial velocities V_a.

surrounding air seems to increase the linear vibration frequency in the supercritical velocity range. The dynamic behaviour changes, however, as the amplitude, and therefore the geometrically nonlinear effect, increases. The fundamental frequency decreases with the influence of the surrounding air, so that given an axial velocity $V_a = 1.4$, the frequency of free vibration at an amplitude of $A/L = 0.01$ is $F = 0.127$ in air whereas it is $F = 0.51$ in a vacuum [3]. The same phenomenon can also be seen in Fig. 8.

The relations between vibration amplitude and axial velocity at different fundamental frequencies are shown in Fig. 7. These are similar to the corresponding ones for a band in a vacuum as seen in Fig. 6 of Ref. [3], so that the nonlinearity bends the curves to the right at subcritical velocities, increasing the axial velocity in very much the same way. The behaviour at low axial velocities and higher amplitudes is also similar. There is a limit on the frequency ($F = 0.221$) beyond which the lower amplitude ranges are not obtainable. The small amplitude vibration, implying linear behaviour, changes only slightly in the supercritical velocity range, but the frequencies of free vibration increase much more rapidly as the axial velocity increases, and an alteration in behaviour occurs as the amplitude, and therefore also the nonlinearity, becomes greater. The nonlinearity seems to compensate for the influence of the surrounding air.

The relation between axial velocity and the fundamental frequency of free vibration both in air and in a vacuum is presented in Fig. 8. In the subcritical velocity range the behaviour is as expected in both cases, the magnitude of the frequencies was reduced to about one fifth due to the surrounding air domain, as in earlier linear studies [5,11,12] and as presented in Fig. 6. The critical velocity increases slightly due to the combined effect of the surrounding air and the geometrical nonlinearity. In the supercritical velocity range, however, the behaviour is complex, being dependent on the extent of nonlinearity; where the change in the fundamental vibration frequency as a function of axial velocity for the band in a vacuum depends only slightly on the amplitude and therefore on the geometrical nonlinearity, this dependence is very strong in the case of a band in air. With small vibration amplitudes, implying linear behaviour, the vibration frequencies increase rapidly as a function of axial velocity, while at increased amplitudes, and at the same time increased geometrical nonlinearity, the slope of the curve tangents decreases markedly so that they are clearly below the values for the vacuum case at near-critical velocities but slope become steeper at increased velocities.

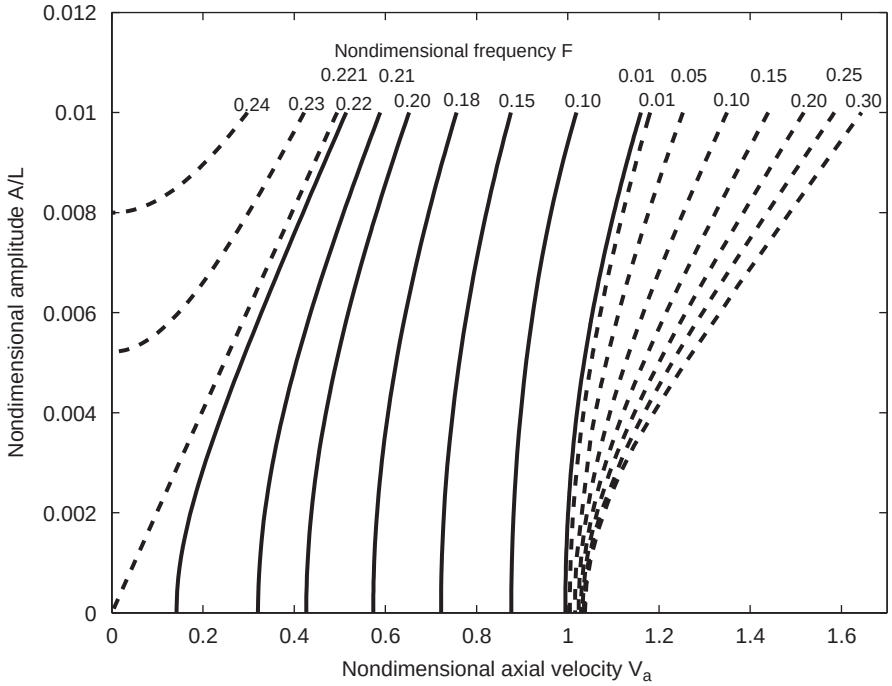

Fig. 7. Non-dimensional amplitude A/L of as a function of non-dimensional axial velocity V with different non-dimensional fundamental frequencies F.

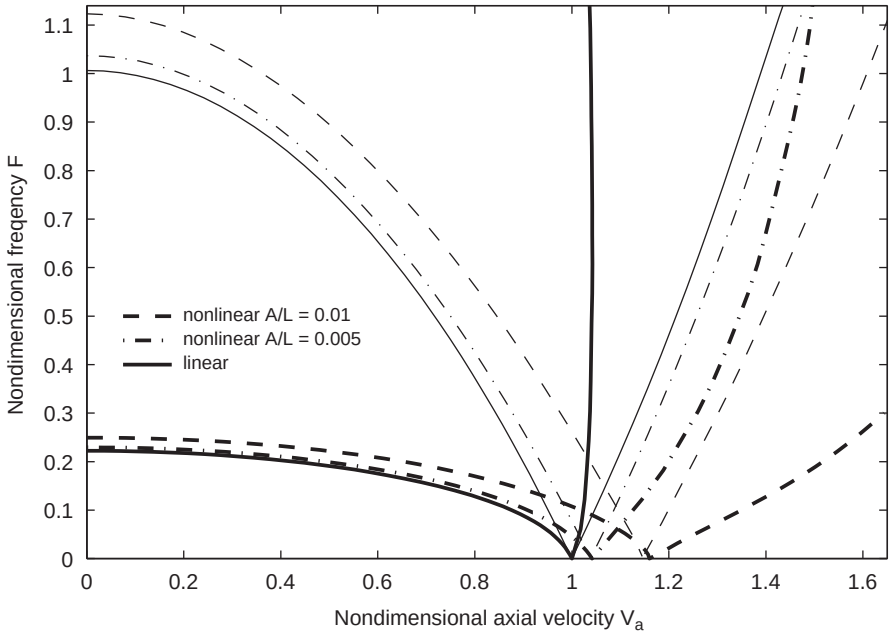

Fig. 8. Non-dimensional fundamental frequency F as a function of non-dimensional axial velocity V_a with different non-dimensional amplitudes A/L. Thick curves present the case in surrounded air and thin curves present the case in a vacuum calculated in Ref. [13].

The vibration modes of the fundamental frequency at three axial velocities and two amplitudes are presented in Fig. 9, the nonlinear $A/L = 0.01$ and the linear $A/L = 0$, except at velocity $V_a = 1.4$, where the lower amplitude is $A/L = 0.0078$. The points of the modes are marked with 'O' in Fig. 6. The modes do not

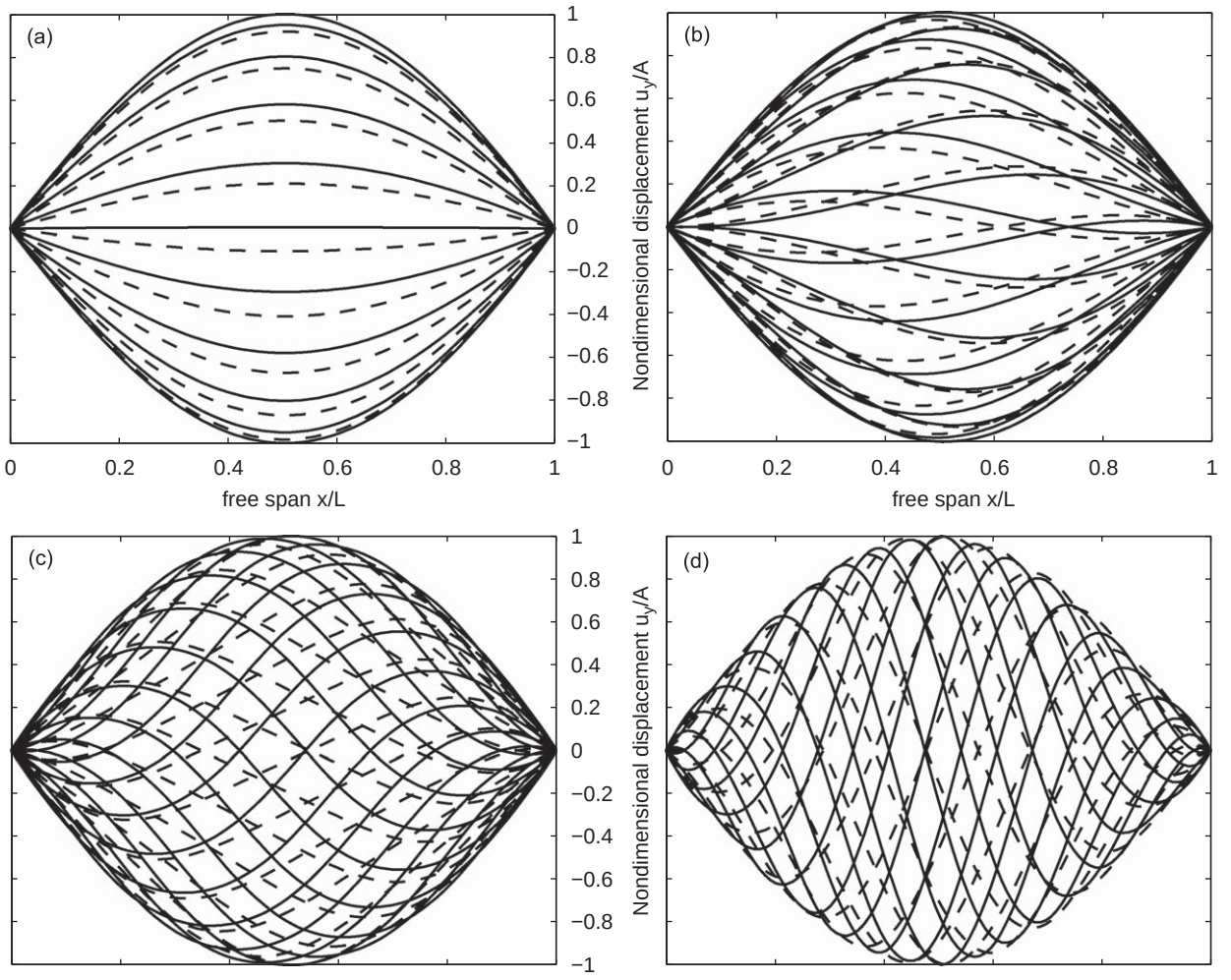

Fig. 9. Deflection shapes of the first mode of an axially moving band at axial velocities: (a) $V_a = 0$, (*b*) $V_a = 0.60$, (c) $V_a = 0.99$ at amplitude $A/L = 0.01$ (- - -) and linear case at $A/L \approx 0$ (—). In (d) $V_a = 1.40$ at amplitude $A/L = 0.01$ (- - -) and at $A/L = 0.0078$ (—).

change so much on account of the surrounding air at subcritical velocities, cf. the modes given in Fig. 9 of Ref. [3], but show the behaviour characteristic of an axially moving material, in that the transverse vibration does not have a constant spatial phase. The phase shift becomes more apparent as the transport velocity increases, and this trend continues into the supercritical speed range. The most notable differences in mode between the cases with and without surrounding air can be found near the critical velocity ($V_a = 0.99$), where the phase shift weakens at higher amplitudes, and at supercritical velocities, where the phase shift strengthens overall.

5. Conclusions

The vibration characteristics of a submerged axially moving band are investigated. A geometrically nonlinear axially moving band model is coupled to the acoustic fluid model and periodic nonlinear problem is solved by the Fourier–Galerkin–Newton (FGN) method. Verification of the model shows that the method is capable of describing the dynamic behaviour of a vibrating system. The nonlinear dynamic behaviour is examined through dependences between fundamental frequency, axial velocity and the amplitude of nonlinear free vibration. The results are compared with the behaviour of the same system in a vacuum as considered in the companion paper [3]. In the subcritical speed range the system behaves as expected in both the linear and

nonlinear case, the effect of the surrounding air field reducing the frequency to about one fifth, as noted in earlier linear studies. The critical velocity itself increases slightly due to combined effect of the surrounding air and the geometrical nonlinearity. In the supercritical speed range the effects of the surrounding air depend on the amplitude of vibration, and therefore on the increase in geometrical nonlinearity. With linear vibrations the fundamental frequency grows faster as a function of axial velocity than in a vacuum, while with nonlinear vibrations the growth in frequency is slower than in a vacuum at near-critical velocities, but with a tendency for a faster increase in frequency at higher velocities.

It should be mentioned that the present investigation was devoted to analysing mainly the influence of aerodynamic loading on geometrically nonlinear vibration in an axially moving band. Further efforts would be needed to study the effects of the nonlinear fluid model and viscous boundary flow.

References

[1] L.-Q. Chen, Analysis and control of transverse vibrations of axially moving strings, *Applied Mechanics Reviews* 58 (2005) 91–116.
[2] M.P. Païdoussis, *Fluid-Structure Interactions. Slender Structure and Axial Flow*, Elsevier Academic Press, London, 2004.
[3] H. Koivurova, The numerical study of the nonlinear dynamics of a light, axially moving string, *Journal of Sound and Vibration* 320 (2009) 373–385.
[4] A. Pramila, Sheet flutter and the interaction between sheet and air, *Tappi Journal* 69 (1986) 70–74.
[5] A. Pramila, Natural frequencies of a submerged axially moving band, *Journal of Sound and Vibration* 113 (1987) 198–203.
[6] Y.B. Chang, S.J. Fox, D.G. Lilley, P.M. Moretti, Aerodynamics of moving belts tapes and webs. *ASME Thirteenth Biennial Conference on Mechanical Vibration and Noise, Symposium on Dynamics of Axially Moving Continua*, Miami, FL, 1991, pp. 33–40.
[7] T. Frondelius, H. Koivurova, A. Pramila, Interaction of an axially moving band and surrounding fluid by boundary layer theory, *Journal of Fluids and Structures* 22 (2006) 1047–1056.
[8] E. Dowell, K. Hall, Modeling of fluid–structure interactions, *Annual Review of Fluid Mechanics* 33 (2001) 445–490.
[9] Y. Lee, Structural-acoustic coupling effect on the nonlinear natural frequency of a rectangular box with one flexible plate, *Applied Acoustics* 63 (2002) 1157–1175.
[10] J. Thomas, E. Dowell, K. Hall, A harmonic balance approach for modeling three-dimensional nonlinear unsteady aerodynamics and aeroelasticity, ASME Paper IMECE-2002-32532, *Proceedings of the ASME International Mechanical Engineering Conference and Exposition*, New Orleans, LA, November, 2002.
[11] J. Niemi, A. Pramila, FEM-analysis of transverse vibration of an axially moving membrane immersed in ideal fluid, *International Journal for Numerical Methods in Engineering* 24 (1987) 2301–2313.
[12] J. Laukkanen, A. Pramila, FEM analysis of a travelling paper web and surrounding air, in: L.A. Godoy, M. Rysz, L.E. Suarrez (Eds.), *Applied Mechanics in the Americas*, Vol. 4, Iowa City, USA, 1997, pp. 505–508.
[13] H. Koivurova, A. Pramila, Nonlinear vibration of axially moving membrane by finite element method, *Computational Mechanics* 20 (1997) 573–581.
[14] A. Kulachenko, P. Gradin, H. Koivurova, Modelling the dynamical behaviour of a paper web—part II, *Computer & Structures* 85 (2007) 148–157.
[15] S. Narayanan, S. Sekar, A frequency domain based numeric–analytical method for nonlinear dynamical systems, *Journal of Sound and Vibration* 211 (1998) 409–424.
[16] O.C. Zienkiewicz, R.L. Taylor, *The Finite Element Method: The basis*, fifth ed., Butterworth-Heinemann, Oxford, 2000.
[17] G.C. Everstine, Finite element formulations of structural acoustics problems, *Computers & Structures* 65 (1997) 307–321.